The existence of five-wave non-collinear acousto-optical weakly coupled states

J. Opt. A: Pure Appl. Opt. **10** (2008) 085106 (10pp) doi:10.1088/1464-4258/10/8/085106

The existence of five-wave non-collinear acousto-optical weakly coupled states

Alexandre S Shcherbakov[1], S E Balderas Mata[1], Je Maximov[2] and A Aguirre Lopez[3,4]

[1] National Institute for Astrophysics, Optics and Electronics, AP 51 y 216, Puebla 72000, Mexico
[2] Molecular Technology GmbH, D-12489 Berlin, Germany
[3] Mixteca University of Technology, Huajuapan de Leon, Oaxaca 69000, Mexico

E-mail: alex@inaoep.mx, smata@inaoep.mx, mtberlin@aol.com and aaguirre@mixteco.utm.mx

Received 8 January 2008, accepted for publication 27 June 2008
Published 21 July 2008
Online at stacks.iop.org/JOptA/10/085106

Abstract
Five-wave Bragg solitary waves in the form of weakly coupled states, occurring within a four-order non-collinear scattering of light by acoustic waves in an optically anisotropic crystal, are identified and investigated. Generally, we study this phenomenon in an arbitrary regime with the phase, i.e. frequency-angular, mismatches, while, for simplicity's sake, the exact conditions appearing of localization for multi-pulse coupled states is illustrated in a regime of the phase synchronism. The spatial-frequency distributions of the optical components inherent in these solitary waves are investigated theoretically, simulated numerically and observed experimentally in a tellurium dioxide crystal. Much attention is given to the analysis of contributions conditioned by the effect of optical activity in a tellurium dioxide crystal of chosen orientation. The performed analysis makes it possible to estimate the effective photo-elastic constants for both normal and anomalous processes of light scattering rather accurately and, in so doing, to match theoretical estimations for the efficiency of multi-order acousto-optical interaction with the experimental results obtained.

Keywords: pulse propagation, solitons, nonlinear optics, parametric processes

(Some figures in this article are in colour only in the electronic version)

1. Introduction

The Bragg scattering of light by acoustic waves in a photo-elastic medium makes possible the origination of multi-wave solitary waves, whose field components differ in physical nature, but are trapped by each other. Such a type of solitary wave, so-called coupled states, have recently been found and investigated in systems with a square-law nonlinearity, namely, in two-mode waveguides [1], where the coupled states could be formed with a collinear geometry of acousto-optical interaction, and in crystals [2], allowing the existence of three- and four-wave coupled states within a non-collinear scattering of light by coherent acoustic phonons. Now we discuss the existence of a new set of solitary waves, representing the most complicated multi-wave acousto-optical coupled states that can be allowed in just the Bragg regime of non-collinear interaction in crystals. These solitary waves include five components and exhibit a property to lock three of their optical components by a pair of the other ones. Here, we develop a quasi-stationary description for such five-wave solitary waves, including both the analytical approach and computer simulation as well as presenting the data obtained due to acousto-optical experiments with a tellurium dioxide crystal (TeO_2).

2. A four-order Bragg scattering of light by acoustic waves in crystals

Strongly nonlinear behavior of light beams with Bragg acousto-optical interaction in a crystal can be easily achieved

[4] Author to whom any correspondence should be addressed.

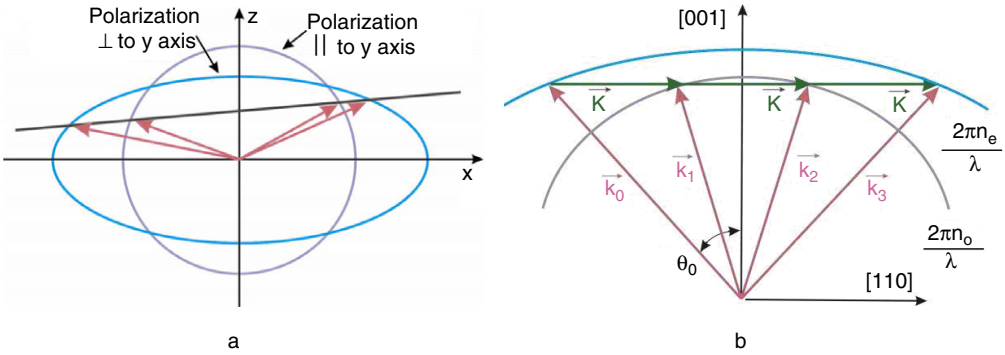

Figure 1. Feasible geometries of acousto-optical interaction in optically anisotropic crystals: an arbitrary case (a) and the particular case of a tellurium dioxide crystal (b).

in an experiment without any observable effect of the scattering process on the acoustic wave, when the powers of the incident light and ultrasound are close to each other, of the order of about 100 mW [3]. In this case, the amplitude of the acoustic wave is governed by a homogeneous wave equation due to a given field approximation, and it is agreed that the regime of so-called weak coupling takes place. Here, we assume that the area of propagation for the acoustic wave, traveling almost perpendicular to the light beams, is bounded by two planes $x = 0$ and L in a crystal, and takes into account both angular and frequency mismatches in the wavevectors. Usually, the Bragg acousto-optical process includes three waves, incident and scattered light modes as well as an acoustic mode, and incorporates conserving both the energy and the momentum for each partial act of a one-phonon scattering. However, if the central cross section of a pair of wavevector surfaces, reflecting two eigenstates of polarization in optically anisotropic media, is crossed by the direct line, placed close enough to a joint center of those surfaces and being collinear to the wavevector of the acoustic beam, one will obtain just four points of intersection, see figure 1(a). This fact indicates that generally the chosen geometry of acousto-optical interaction in anisotropic media allows, as a maximum, a four-order scattering of light by acoustic waves in the Bragg regime and in so doing represents the most complicated case of just the Bragg non-collinear acousto-optical interaction in crystals. In this particular case, when these four intersections are equidistant, a four-order scattering of light can be provided by only one harmonic acoustic wave, as shown for a tellurium dioxide crystal in figure 1(b). By this is meant that, under certain conditions, i.e. at a set of angles of light incidence on the selected crystal cut and at fixed frequency of the acoustic wave, one will be able to observe the Bragg scattering of light caused by sequential participation of one, two or even three phonons. Consequently, four light modes and one acoustic mode will interact with each other.

The conservation laws are given by $\omega_1 = \omega_0 + \Omega$, $\vec{k}_1 = \vec{k}_0 + \vec{K}$, $\omega_2 = \omega_0 + 2\Omega$, $\vec{k}_2 = \vec{k}_0 + 2\vec{K}$, $\omega_3 = \omega_0 + 3\Omega$ and $\vec{k}_3 = \vec{k}_0 + 3\vec{K}$ simultaneously (ω_p, $\vec{k}_p$ and Ω, $\vec{K}$ are the cyclic frequencies and the wavevectors of light and acoustic waves, $p = 0, 1, 2, 3$). Such a five-wave process appears at the angle θ_0 of light incidence and the frequency Ω_0, peculiar to just a four-order Bragg scattering of light, which can be found from figure 1(b) as [4] $\sin\theta_0 = 3(4n_0)^{-1}\sqrt{2|n_e^2 - n_0^2|}$ and $\Omega_0 = 2\pi f_0 = \pi v\lambda^{-1}\sqrt{2|n_e^2 - n_0^2|}$, where $n_0 \neq n_e$ are the refractive indices of a crystal ($n_0 < n_e$ in a tellurium dioxide crystal), v is the ultrasound velocity and λ is the incident light wavelength.

The polarizations of light in the zero and third orders of scattering are orthogonal to the polarizations in the first and second orders, whereas the frequencies of light beams in the first, second and third orders are shifted by Ω_0, $2\Omega_0$ and $3\Omega_0$, respectively, relative to the zero-order beam. A set of equations for the normalized amplitudes $C_p(x)$ of light waves with the stationary four-order light scattering in the Bragg regime is given by [4]

$$\begin{aligned}
\frac{\mathrm{d}C_0}{\mathrm{d}x} &= -q_a C_1 \exp(-\mathrm{i}\eta_0 x)\,,\\
\frac{\mathrm{d}C_1}{\mathrm{d}x} &= q_a C_0 \exp(\mathrm{i}\eta_0 x) - q_n C_2 \exp(-\mathrm{i}\eta_1 x)\,,\\
\frac{\mathrm{d}C_2}{\mathrm{d}x} &= q_n C_1 \exp(\mathrm{i}\eta_1 x) - q_a C_3 \exp(-\mathrm{i}\eta_2 x)\,,\\
\frac{\mathrm{d}C_3}{\mathrm{d}x} &= q_a C_2 \exp(\mathrm{i}\eta_2 x)\,.
\end{aligned} \tag{1}$$

The parameters $\eta_p = k_{p,x} - k_{p+1,x}$, explained in terms of x components for the scattered light wavevectors, represent the joint angular-frequency mismatches. The factors q_n and q_a describe both the material properties relative to normal and anomalous processes of light scattering and the acoustic power densities; they are independent of x. Generally $q_n \neq q_a$, because these factors include different components of the photo-elastic tensor inherent in a crystal. In fact, these factors are given by

$$\begin{aligned}
q_n &= \frac{\pi}{\lambda} p_{\mathrm{n,eff}} \sqrt{\frac{P n_0^6}{2\rho_0 v^3}},\\
q_a &= \frac{\pi}{\lambda} p_{\mathrm{a,eff}} \sqrt{\frac{P n_0^3 n_e^3}{2\rho_0 v^3}},
\end{aligned} \tag{2}$$

where P is the acoustic power density, ρ_0 is the material density of a crystal, and $p_{\mathrm{n,eff}}$ and $p_{\mathrm{a,eff}}$ are the effective photo-elastic constants for normal and anomalous regimes of light

scattering, respectively. The principal magnitudes N_e and N_0 of the refractive indices n_e and n_0 are rather close to each other in a tellurium dioxide crystal. For example, $N_e = 2.41$, $N_0 = 2.26$ at $\lambda = 633$ nm and $N_e = 2.49$, $N_0 = 2.33$ at $\lambda = 488$ nm [5], so that one can estimate $n_0^{3/2} \approx n_e^{3/2}$ and $q = q_a/q_n \approx p_{\mathrm{a,eff}}/p_{\mathrm{n,eff}}$ with an error of about 7%. Now, however, the main attention should be paid to determining the specific magnitude of the ratio q for a tellurium dioxide crystal. In so doing, one has to consider the photo-elastic properties of this crystal, taking into account the effect of optical activity.

3. Five-wave non-collinear weakly coupled acousto-optical states

We take equation (1) with the simplest boundary conditions $|C_0(x=0)|^2 = I^2$, $C_{1,2,3}(x=0) = 0$ and exploit the conservation law $|C_0|^2 + |C_1|^2 + |C_2|^2 + |C_3|^2 = I^2$, resulting from equation (1), where I^2 is the intensity of the continuous-wave incident light beam. The complete analytical solution to equation (1) is too unwieldy, so at first we assume that $\eta_0 = \eta_1 = \eta_2 = 0$ which yields

$$C_0(q_n x) = \frac{I}{2\sqrt{1+4q^2}}\left[\left(-2q^2+P^2\right)\cos\left(\frac{Sq_n x}{\sqrt{2}}\right) + \left(2q^2-S^2\right)\cos\left(\frac{Pq_n x}{\sqrt{2}}\right)\right], \tag{3}$$

$$C_1(q_n x) = \frac{I}{2q\sqrt{2(1+4q^2)}}\left[P\left(2q^2-S^2\right)\sin\left(\frac{Sq_n x}{\sqrt{2}}\right) + S\left(-2q^2+P^2\right)\sin\left(\frac{Pq_n x}{\sqrt{2}}\right)\right], \tag{4}$$

$$C_2(q_n x) = \frac{qI}{\sqrt{1+4q^2}}\left[\cos\left(\frac{Sq_n x}{\sqrt{2}}\right) - \cos\left(\frac{Pq_n x}{\sqrt{2}}\right)\right], \tag{5}$$

$$C_3(q_n x) = \frac{I}{\sqrt{2(1+4q^2)}}\left[P\sin\left(\frac{Sq_n x}{\sqrt{2}}\right) - S\sin\left(\frac{Pq_n x}{\sqrt{2}}\right)\right], \tag{6}$$

where

$$P = \sqrt{1+2q^2+\sqrt{1+4q^2}} \quad \text{and} \quad S = \sqrt{1+2q^2-\sqrt{1+4q^2}}.$$

As follows from equations (3)–(6), the light intensities $|C_p(x)|^2$ are periodic in the coordinate x, so such values $x_n \neq 0$ exist that $|C_0(x_n)|^2 = I^2$, $C_{1,2,3}(x_n) = 0$ with $n = 1, 2, \ldots$. Thus, when $x = x_n$, the intensities in a triplet of the scattered light waves become zero outside the area occupied by the acoustic wave, i.e. the phenomenon of localization appears for the above-listed optical scattered components. Inside that area, the spatial distributions of the scattered light waves contain a number of peaks and holes, and simultaneously the corresponding distribution of the incident light wave has holes or peaks at the same spatial positions. Equations (3)–(6) give us an opportunity to search for completely localized distributions of the scattered optical components with $\eta_0 = \eta_1 = \eta_2 = 0$, i.e. in the case of exact phase synchronism. Broadly speaking, this problem can be formulated in various ways, and we consider here the simplest case. Namely, we assume that the completely localized distributions are associated with the relations $C_0(q_n L) = \pm I$, while $C_1(q_n L) = C_2(q_n L) = C_3(q_n L) = 0$, where $L \in \{x_n\}$ is the spatial length of localization. Let us start with equation (5) which is the simplest one in a set. The relation $C_2(q_n L) = 0$ leads to the formula $\cos(Sq_n x/\sqrt{2}) = \cos(Pq_n x/\sqrt{2})$, but the obvious analysis shows that only the case of $\cos(Sq_n x/\sqrt{2}) = \cos(Pq_n x/\sqrt{2}) = \pm 1$ gives us an opportunity to retain freedom in determining both the parameters P and S as well as the length L. The last formula provides the existence of all the above-listed localized distributions and converts the associated relations into trivial equalities. That is why we arrive at two triplets of the localization conditions. The first triplet is given by $q_n L = 2\sqrt{2}\pi k/S = 2\sqrt{2}\pi m/P$, where k and m are whole numbers; $m > k$, because $P > S$. If $k = 0$, we yield $m = 0$ and $q_n L = 0$, which is trivial. So, we put $k \neq 0$ and, using the parameters P and S, obtain the formula

$$m\sqrt{1+2q^2-\sqrt{1+4q^2}} = k\sqrt{1+2q^2+\sqrt{1+4q^2}}, \tag{7}$$

correlating the whole numbers k and m and the parameter q in the first triplet. The second triplet can be written as $q_n L = \sqrt{2}(\pi + 2\pi k)/S = \sqrt{2}(\pi + 2\pi m)/P$. Here, $m > k$ as well, but the value of $k = 0$ is now acceptable. The interrelation between the whole numbers k and m and the parameter q is now given by

$$(1+2m)\sqrt{1+2q^2-\sqrt{1+4q^2}} = (1+2k)\sqrt{1+2q^2+\sqrt{1+4q^2}}. \tag{8}$$

Two diagrams in figure 2, reflecting equations (7) and (8), depict various interplays between the whole number m and the parameter q for a set of whole numbers k. The solutions to equations (7) and (8) are presented by intersections of the curves with the fixed numbers k and the horizontal lines with the fixed numbers m. Some of the intersections lead to the same solutions with different values $q_n L$, so the minimal value of $q_n L$ will be realized in such cases.

The corresponding exactly localized distributions for the intensities $|C_p(x)|^2$ of optical components inherent in the system, described by a set of equations (3)–(6) with various values of the parameter q on the interval $q_n L \in [0, 4\pi]$, are shown in figure 3.

It is clearly seen that these spatial distributions represent multi-pulse dark solitary waves in zero order together with bright solitary waves in first, second and third orders of scattering. These results make it possible to conclude that the Bragg solitary waves in the form of five-wave weakly coupled acousto-optical states exist under the localization conditions, see equations (7) and (8), on a discrete totality of points in a three-dimensional (k, m, q)-space.

4. Optical activity in a tellurium dioxide single crystal

In the optics of crystals, it is worthwhile to analyze the dependence of the electric field strength $\vec{E}(\vec{r}, t)$ on the electric

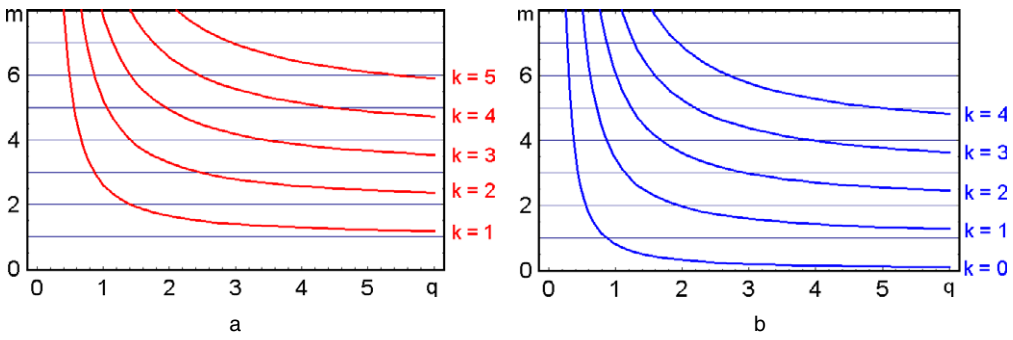

Figure 2. Graphical interpretation of the localization conditions: (a) for equation (7), (b) for equation (8).

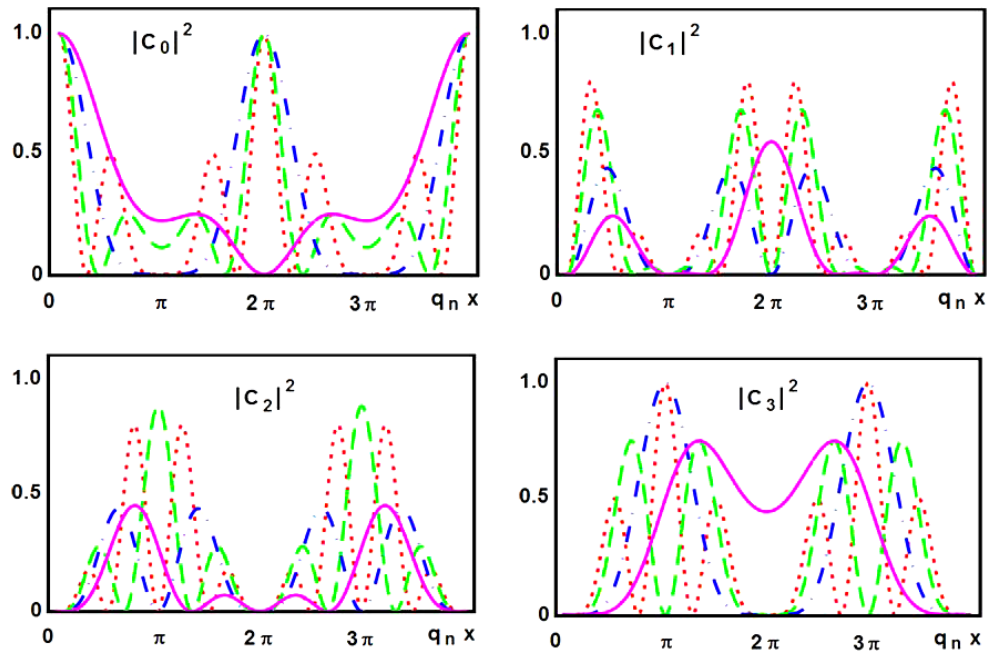

Figure 3. Distributions for the optical components: the red (dotted) lines are for $q = 1.936$, the green (dashed) lines are for $q = 1.414$, the blue (dotted-dashed) lines are for $q = 0.866$ and the violet (solid) lines are for $q = 0.559$.

field induction $\vec{D}(\vec{r}, t)$, which has the form $\vec{E}(\vec{r}, t) = \kappa \vec{D}(\vec{r}, t)$ in the local case, where κ is the dielectric impermeability tensor whose eigenvalues are inverse squares of the main refractive indices inherent in a crystal. However, sometimes crystals are characterized by the spatial non-locality and exhibit spatial dispersion. Effect of the optical activity can be observed in crystals, which exhibit a dependence on the first spatial derivatives of the electric field induction $\vec{D}(\vec{r}, t)$, so that in the first approximation one can write $\vec{E}(\vec{r}, t) = \kappa \vec{D}(\vec{r}, t) + g[\partial \vec{D}(\vec{r}, t)/\partial \vec{r}]$, where $g \neq 0$. Due to $\partial \vec{D}(\vec{r}, t)/\partial \vec{r} = \mathrm{i}\vec{k}\vec{D}$ for the monochromatic plane light wave with the wavevector $\vec{k}$, we yield $E_j = (\kappa_{jl} + \mathrm{i}g_{jlm}k_m)\ D_l$. The expression in brackets is a modified tensor of the dielectric impermeability whose corrections have an order of the ratio a/λ, where a is the atomic cell size in a crystal, λ is the light wavelength corresponding to the wavevector $\vec{k} = (2\pi/\lambda)\vec{m}$ and $\vec{m}$ is the unit vector of the wave normal. If the crystal is optically transparent, a modified tensor of the dielectric impermeability is Hermitian, so that its real-valued part is symmetrical and its imaginary-valued part is anti-symmetrical in behavior. Thus, the tensor g is anti-symmetrical in the first pair of indices, i.e. $g_{jlm} = -g_{ljm}$, while the pseudo-tensor G, being dual to the tensor g with an accuracy of the factor $\lambda/(2\pi)$, can be introduced as $G_{\ln} = \pi\lambda^{-1}\delta_{jkl}g_{kjn}$, where $\delta_{jkl} = (1/2)(j-k)(k-l)(l-j)$ is the unit anti-symmetric Levi-Civita tensor. Consequently, one can rewrite $E_j = (\kappa_{jl} + \mathrm{i}\delta_{jlm}G_{mn}m_n)D_l$. Then, let us take the coordinate system whose axes X_1 and X_2 are oriented along the main axes of a crystal, while $X_3 \parallel \vec{m}$. In these coordinates

$$E_1 = n_{01}^{-2}D_1 + \mathrm{i}G_{33}D_2, \qquad E_2 = n_{02}^{-2}D_2 - \mathrm{i}G_{33}D_1, \tag{9}$$

because $D_3 = 0$, $\kappa_{12} = 0$, $\kappa_{11} = n_{01}^{-2}$ and $\kappa_{22} = n_{02}^{-2}$. Here, n_{01} and n_{02} are the refractive indices for light waves in the absence of spatial dispersion and $n_{01} \gtrless n_{02}$. The Maxwell's equations for the plane waves require $\vec{E} - \vec{m}\vec{m} \cdot \vec{E} = n^{-2}\vec{D}$. In the chosen coordinate system, it leads to $E_{1,2} = n^{-2}D_{1,2}$. Exploiting these relations, one can exclude the values $E_{1,2}$

from equation (9), write a set of two homogeneous equations for the values $D_{1,2}$ and obtain the characteristic equation for that set in the form of $(n_{01}^{-2} - n^{-2})(n_{02}^{-2} - n^{-2}) - G_{33}^2 = 0$. Solving this algebraic equation relative to n and taking into account that $|G_{33}| \ll n_{01}, n_{02}$, one can find that

$$\begin{aligned} n_1 &= n_{01} + \tfrac{1}{2} n_{01}^3 \rho G_{33}, \\ n_2 &= n_{02} - \tfrac{1}{2} n_{02}^3 \rho G_{33}, \end{aligned} \tag{10}$$

$$\rho = \frac{1}{2G_{33}} \left[\sqrt{(n_{02}^{-2} - n_{01}^{-2})^2 + (2G_{33})^2} - (n_{02}^{-2} - n_{01}^{-2}) \right]. \tag{11}$$

Here, $|\rho| \leqslant 1$ due to $n_{01} \geqslant n_{02}$ and $\operatorname{sign} \rho = \operatorname{sign} G_{33}$. The obtained relations give the possibility for considering the important regime when the wave normal $\vec{m}$ is oriented close to the optical axis of a uniaxial crystal. If $\vec{m}$ is parallel to the optical axis, we have $n_{01} = n_{02} = N_0$ (where N_0 is the main refractive index for the ordinary light wave) and $\rho = \operatorname{sign} G_{33}$, so that two circularly polarized light wave pass along the optical axis and equations (10) take the forms

$$\begin{aligned} n_1 &= N_0 + \tfrac{1}{2} N_0^3 \, |G_{33}| \, , \\ n_2 &= N_0 - \tfrac{1}{2} N_0^3 \, |G_{33}| \, . \end{aligned} \tag{12}$$

Just these formulae describe the plots for cross sections of the refractive index surfaces in the vicinity of an optical axis inherent in the tellurium dioxide crystal, which was shown in figure 1(b). If the birefringence of the crystal is not very small, the parameter ρ decreases with deviating wave normal $\vec{m}$ from the optical axis by the angle ϑ. When $(n_{02}^{-2} - n_{01}^{-2})^2 \approx (2G_{33})^2$ in equation (11), we yield $|\rho| = \sqrt{2} - 1 \approx 0.4$. One can calculate that this value of ρ leads to the expression $\sin \vartheta = \sqrt{|2G_{33}(N_e^{-2} - N_0^{-2})^{-1}|}$, where N_e is the main refractive index for the extraordinary light wave. Usually, $G_{33} \approx 10^{-4}$–10^{-5} and $(N_e^{-2} - N_0^{-2}) \approx 0.02$–$0.06$: therefore the angle ϑ is about a few degrees. In practice, the value of G_{33} can be determined experimentally through measuring the specific rotation of the polarization when a light beam of wavelength λ is passing along the optical axis of a crystal, because $G_{33} = \lambda\alpha/(\pi N_0^3)$. One can estimate G_{33} for a TeO_2 crystal from [5] and equation (12), so that: (1) $G_{33} = 2.83 \times 10^{-5}$, $N_0 = 2.2597$, $N_e = 2.4119$ at $\lambda = 633$ nm; (2) $G_{33} = 4.26 \times 10^{-5}$, $N_0 = 2.3297$, $N_e = 2.4951$ at $\lambda = 488$ nm; and (3) $G_{33} = 5.60 \times 10^{-5}$, $N_0 = 2.3511$, $N_e = 2.5306$ at $\lambda = 442$ nm.

5. Polarization of light waves and its ellipticity in a tellurium dioxide single crystal

A rather general form for a pair of electric induction vectors $\vec{D}^{(1,2)}(\vec{r}, t)$, passing through a crystal, is given by

$$\begin{aligned} \vec{D}^{(1)} &= D^{(1)} \, (\vec{e}_1 + \mathrm{i}\rho\vec{e}_2) \exp\left[\mathrm{i} \, (k_1 x_3 - \omega t + \varphi_1)\right], \\ \vec{D}^{(2)} &= D^{(2)} \, (\mathrm{i}\rho\vec{e}_1 + \vec{e}_2) \exp\left[\mathrm{i} \, (k_2 x_3 - \omega t + \varphi_2)\right], \end{aligned} \tag{13}$$

where $D^{(\alpha)} \exp[\mathrm{i}\varphi_{(\alpha)}]$ are the complex amplitudes, $k_{(\alpha)} = \omega n_{(\alpha)}/c$ and $\alpha = 1, 2$. Here, ρ is the measure of ellipticity for the polarization state, so that $\rho = 0$ for the linear polarization and $\rho = \pm 1$ for the circular polarization, right or left. It follows from equations (13) that the vectors of polarization have the form

$$\begin{aligned} \vec{e}_1 + \mathrm{i}\rho\vec{e}_2 &= \begin{pmatrix} 1 \\ \mathrm{i}\rho \end{pmatrix}, \\ \mathrm{i}\rho\vec{e}_1 + \vec{e}_2 &= \begin{pmatrix} \mathrm{i}\rho \\ 1 \end{pmatrix}. \end{aligned} \tag{14}$$

Their moduli can be calculated as

$$\begin{aligned} (\vec{e}_1 - \mathrm{i}\rho\vec{e}_2)\,(\vec{e}_1 + \mathrm{i}\rho\vec{e}_2) &= (1, -\mathrm{i}\rho) \begin{pmatrix} 1 \\ \mathrm{i}\rho \end{pmatrix} = 1 + \rho^2, \\ (-\mathrm{i}\rho\vec{e}_1 + \vec{e}_2)\,(\mathrm{i}\rho\vec{e}_1 + \vec{e}_2) &= (-\mathrm{i}\rho, 1) \begin{pmatrix} \mathrm{i}\rho \\ 1 \end{pmatrix} = \rho^2 + 1. \end{aligned} \tag{15}$$

Using equations (15), one can normalize the vectors in equation (14) by $\sqrt{1 + \rho^2}$ and write the unit vectors of polarization as

$$\begin{aligned} \vec{\nu}_1 &= \left(1 + \rho^2\right)^{-1/2} (\vec{e}_1 + \mathrm{i}\rho\vec{e}_2) \, , \\ \vec{\nu}_2 &= \left(1 + \rho^2\right)^{-1/2} (\mathrm{i}\rho\vec{e}_1 + \vec{e}_2) \, . \end{aligned} \tag{16}$$

The scalar products $\vec{\nu}_1^{+}\vec{\nu}_2 = \vec{\nu}_2^{+}\vec{\nu}_1 = 0$ illustrate the mutual orthogonality of these unit vectors.

The main formula for the ellipticity of light polarization is equation (11). Tellurium dioxide is a uniaxial crystal, so that $n_{02} = N_0$ is the main refractive index for the ordinary state of polarization, while $n_{01} = n_e(x, z)$ depends on the direction (x, z) in a crystal and has the form of an ellipse $\frac{x^2}{N_e^2} + \frac{z^2}{N_0^2} = 1$. We are interested in rather small tips from the [001] $\parallel z$ axis. Therefore, one can consider the coordinates (x_0, z_0) of a cross-point of this ellipse with a direct line $x = z \tan(\pi\vartheta/180)$ when the angle ϑ of the tip from the [001] axis is measured in angular degrees. In fact, one needs the length of the linear segment between the origin of the coordinates and this cross-point. These coordinates are given by

$$\begin{aligned} x_0 &= \frac{N_e N_0 \tan(\pi\vartheta/180)}{\sqrt{N_e^2 + N_0^2 \tan^2(\pi\vartheta/180)}}, \\ z_0 &= \frac{N_e N_0}{\sqrt{N_e^2 + N_0^2 \tan^2(\pi\vartheta/180)}}, \end{aligned} \tag{17}$$

and consequently

$$n_e^2 = x_0^2 + z_0^2 = \frac{N_e^2 N_0^2 [1 + \tan^2(\pi\vartheta/180)]}{N_e^2 + N_0^2 \tan^2(\pi\vartheta/180}) \geqslant n_0^2 \equiv N_0^2. \tag{18}$$

Finally, one can write

$$\rho(\vartheta) = \frac{1}{2G_{33}} \left[\sqrt{(N_0^{-2} - n_e^{-2})^2 + (2G_{33})^2} - (N_0^{-2} - n_e^{-2}) \right]. \tag{19}$$

Dependences of the ellipticity ρ of polarization for the light waves versus the angle ϑ of deflection from the [001] axis in a TeO_2 crystal for a few light wavelengths are depicted

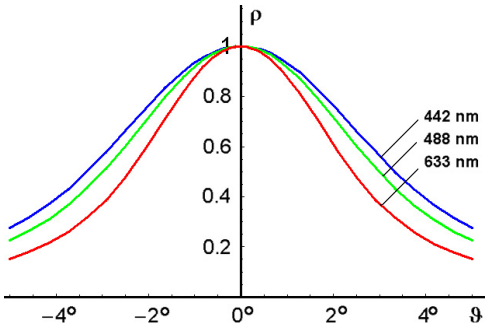

Figure 4. The ellipticity ρ of polarization of the light waves versus the angle ϑ of a tip from the [001] axis in a TeO_2 crystal.

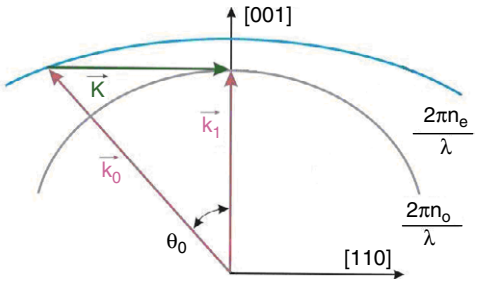

Figure 5. A wide-band geometry for the anomalous regime of light scattering in a TeO_2 crystal.

in figure 4. Physically, possible magnitudes of the angle ϑ coincide with the angles θ of incidence or scattering the light beams as $\theta = \vartheta$. The estimations, performed for a tellurium dioxide crystal for the above-discussed orientation, show that the normal regime of light scattering (using the ordinary state of polarization) meets: (1) $\theta = 0.786°$ at $\lambda = 633$ nm, $f = 60$ MHz; (2) $\theta = 0.657°$ at $\lambda = 488$ nm, $f = 67$ MHz; and (3) $\theta = 0.505°$ at $\lambda = 442$ nm, $f = 58$ MHz. With regard to the optimized anomalous regime of light scattering, it is worthwhile to consider the particular case of a geometry presented in figure 5, because such a geometry provides the most wide-band acousto-optical interaction with polarization rotation [6]. This geometry requires a specific magnitude f_0 of elastic wave frequency, but can lead to manifesting two-phonon light scattering [3, 4] by applying a rather powerful acoustic signal to a cell. Under this restricting condition of a small enough acoustic signal, one can calculate that the angles of light incidence are determined by $\sin\theta_0 \approx \theta_0 = \lambda f_0/(n_0 V)$, so that: (1) $\theta_0 = 0.919°$ at $\lambda = 633$ nm, $f_0 = 37.4$ MHz; and (2) $\theta_0 = 1.132°$ at $\lambda = 488$ nm, $f_0 = 63.3$ MHz. The angles of scattering in this regime are definitely smaller than the values of θ_0, as follows from figure 4. Thus, the obtained estimations for angles show that the range of varying these angles lies approximately in a limit of 0.5°–1.5°. Therefore, the angular dependence for the ellipticity ρ of polarization in figure 4 is perfectly adequate for the real situation in a tellurium dioxide single crystal. Consequently, the magnitudes of ρ lie in their turn between 0.75 and 0.97 in the visible optical range, as can be concluded from figure 4, and moreover the magnitude of ρ grows as the light wavelength decreases.

6. Photo-elastic effect in a tellurium dioxide single crystal

Generally, when the elastic wave is passing through a medium, the dielectric impermeability tensor $\hat{\kappa}$ becomes perturbed under the action of mechanical deformations $\hat{\gamma}$ and takes the form $\hat{\kappa} + \hat{\zeta}$, where the symmetrical tensor $\hat{\zeta} = \hat{p}\hat{\gamma}$ of the second rank presents small corrections to the tensor $\hat{\kappa}$ and $\hat{p}$ is the tensor of the fourth rank of photo-elastic coefficients [7]. In the particular case of a TeO_2 crystal (its point symmetry group is 422), when the slowest shear acoustic wave is passing along the $[1\bar{1}0]$ axis of that crystal and the displacement vector is oriented along the [110] axis, one can find

$$\zeta_{ij} = p_{ijkl}\gamma_{kl} = \tfrac{1}{2}(p_{11} - p_{12}) \begin{pmatrix} 1 & 0 & 0 \\ 0 & -1 & 0 \\ 0 & 0 & 0 \end{pmatrix}. \qquad (20)$$

Then, it is well known that physical axes of the optical indicatrix determine orientations for a pair of eigenvectors of the electric induction in a crystal. That is why the quadratic form $p_{\text{eff}} = d_i^{(s)}\zeta_{ij}d_j^{(i)}$ describes the effective photo-elastic constant p_{eff} of the scattering process, i.e. the efficiency of converting the initial state of light polarization, described by the unit vector $\vec{d}^{(i)}$ oriented along the corresponding electric induction vector $\vec{D}^{(i)}$ into the scattered state of light polarization, characterized by the unit vector $\vec{d}^{(s)}$ oriented along the corresponding electric induction vector $\vec{D}^{(s)}$ due to the photo-elastic effect (or, which is the same, the acousto-optical interaction) in a crystal.

Now, the eigenstate unit vectors of polarization can be applied to estimating the scattering photo-elastic properties of a TeO_2 crystal for the above-mentioned crystalline orientation. These unit vectors are given by equation (16). One may exploit a two-dimensional reduced version of the correction matrix $\tilde{\zeta}_{ij}$ to the dielectric impermeability tensor $\hat{\kappa}$ instead of equation (20), which is additionally normalized by the factor $(p_{11} - p_{12})/2$. It can be done, because all the angles of incidence and scattering are rather small, lie in the range of 0.5°–1.5° (see the previous section) and definitely do not exceed two angular degrees. Such an approximation implies that only the ellipticity ρ reflects the measure of angular deflection from the optical axis for all the light beams in a crystal. The matrix of corrections represents a minor of the matrix ζ_{ij} and has the form $\hat{\zeta}_{ij} = \begin{pmatrix} 1 & iG_{33} \\ -iG_{33} & -1 \end{pmatrix}$, where contributions of the optical activity are taken into account. Thus, in the regime with conserving the polarization state, i.e. with the normal regime of light scattering, one can find

$$\begin{aligned} \hat{p}_{\text{eff}}(1 \to 1) &= \vec{v}_1^{+}\hat{\zeta}_{ij}\vec{v}_1 = \frac{1 - \rho^2 - 2\rho G_{33}}{1 + \rho^2}, \\ \hat{p}_{\text{eff}}(2 \to 2) &= \vec{v}_2^{+}\hat{\zeta}_{ij}\vec{v}_2 = \frac{\rho^2 - 1 + 2\rho G_{33}}{1 + \rho^2}. \end{aligned} \qquad (21)$$

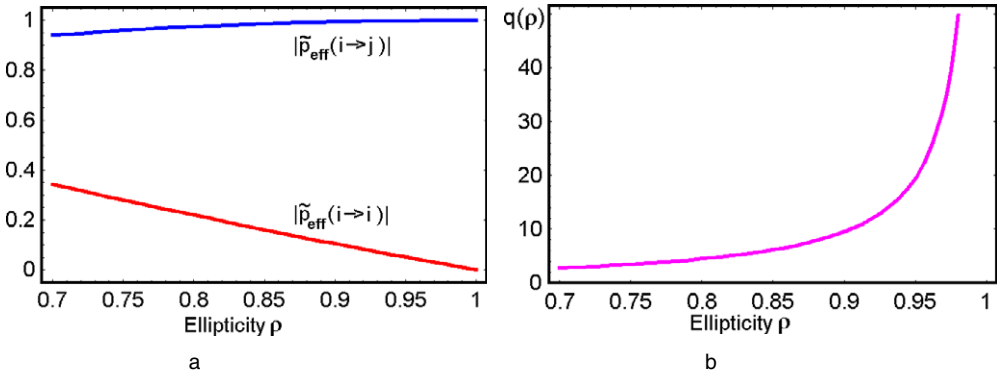

Figure 6. Moduli of the normalized effective photo-elastic constants $|\tilde{p}_{\rm eff}(i \to i)|$ and $|\tilde{p}_{\rm eff}(i \to j)|$ (a) and their ratio q (b) versus the ellipticity ρ of the eigenstates of polarization in a TeO_2 crystal, see equations (23).

In the regime with changing the polarization state, i.e. with the anomalous regime of scattering, one can obtain

$$\begin{aligned}\hat{p}_{\rm eff}(1 \to 2) &= \vec{\nu}_2^{+}\hat{\zeta}_{ij}\vec{\nu}_1 \\ &= \frac{-2{\rm i}\rho - {\rm i}(1-\rho^2)G_{33}}{1+\rho^2}\exp\left[{\rm i}\,(\varphi_1 - \varphi_2)\right], \\ \hat{p}_{\rm eff}(2 \to 1) &= \vec{\nu}_1^{+}\hat{\zeta}_{ij}\vec{\nu}_2 \\ &= \frac{2{\rm i}\rho + {\rm i}(1-\rho^2)G_{33}}{1+\rho^2}\exp\left[{\rm i}\,(\varphi_2 - \varphi_1)\right].\end{aligned} \tag{22}$$

Starting our estimations from equations (21) one has to compare the summands $|1-\rho^2|$ and $|2\rho G_{33}|$ with each other. In the worst case of the smallest angle $\vartheta = 0.5°$, one can take: (1) $\rho = 0.97$, $G_{33} = 5.60 \times 10^{-5}$ and find $|1-\rho^2| = 0.059\,10$, $|2\rho G_{33}| = 0.000\,11$ at $\lambda = 442$ nm; and (2) $\rho = 0.96$, $G_{33} = 2.83 \times 10^{-5}$ and calculate $|1-\rho^2| = 0.078\,41$, $|2\rho G_{33}| = 0.000\,05$ at $\lambda = 633$ nm. These estimations show that $|2\rho G_{33}| \ll |1-\rho^2|$ in a TeO_2 crystal, so that in practice the term $2\rho G_{33}$ can be omitted in equations (21). Then, one has to compare with each other the summands $|2\rho|$ and $|(1-\rho^2)G_{33}|$ in equations (22). Within these estimations, the worst case is associated with the largest angle $\vartheta = 1.5°$ and one can take: (1) $\rho = 0.85$, $G_{33} = 5.60 \times 10^{-5}$ and find $|(1-\rho^2)G_{33}| = 0.000\,016$, $|2\rho| = 1.700\,000$ at $\lambda = 442$ nm; and (2) $\rho = 0.75$, $G_{33} = 2.83 \times 10^{-5}$ and calculate $|(1-\rho^2)G_{33}| = 0.000\,012$, $|2\rho| = 1.500\,000$ at $\lambda = 633$ nm. These calculations demonstrate that $|(1-\rho^2)G_{33}| \ll |2\rho|$ in a TeO_2 crystal, and again in practice the term $(1-\rho^2)G_{33}$ can be omitted in equations (22). Finally, let us use the reduced versions of equations (21) and (22) to estimate the modulus of the normalized effective photo-elastic constants in terms of the eigenstates of polarization as

$$\begin{aligned}|\tilde{p}_{\rm eff}(i \to i)| &= \left|\frac{1-\rho^2}{1+\rho^2}\right|, \\ |\tilde{p}_{\rm eff}(i \to j)| &= \left|\frac{2\rho}{1+\rho^2}\right|, \\ q\,(\rho) = \frac{|\tilde{p}_{\rm eff}(i \to j)|}{|\tilde{p}_{\rm eff}(i \to i)|} &= \left|\frac{2\rho}{1-\rho^2}\right|,\end{aligned} \tag{23}$$

where $(i, j) = (1, 2)$. One can see that $|\tilde{p}_{\rm eff}(i \to i)| < |\tilde{p}_{\rm eff}(i \to j)|$ with $\rho \in [0.7, 1.0]$, for example, $q(\rho) \approx 4.44$ with $\rho = 0.8$. The results of the corresponding numerical estimations for the ellipticity ρ lying between 0.70 and 0.97 are presented in figure 6. One can see that generally the efficiency of anomalous light scattering exceeds significantly the efficiency of normal scattering in a TeO_2 crystal under the selected orientation of this crystal in a cell, so that $q(\rho) > 1$.

It is well known [4, 5] that the anomalous regime in a TeO_2 crystal with the crystallographic orientation under consideration is characterized by extremely high efficiency due to $p_{\rm eff,an} = 0.5(p_{11} - p_{12})$ and $M_2 = 1.2 \times 10^{-15}$ s^3 g^{-1}. In contrast, the theoretically predicted magnitude of the effective photo-elastic constant $p_{{\rm eff},n}$ in the normal regime is much smaller than $p_{\rm eff,an}$ in the case of the same orientation for a crystal. For example, recent experimental data [8, 9] give the ratio $p_{{\rm eff},n} \leqslant 0.1\,p_{\rm eff,an}$.

7. Five-wave non-collinear weakly coupled acousto-optical states in a TeO_2 crystal

Now we take into account the mismatches, assume the precise angular alignment of a cell and extend η_0, η_1 and η_2 into a power series only in terms of the frequency detuning $\Delta f = |f - f_0|$ for the current frequency f relative to the frequency f_0 of exact synchronism. In the first approximation on Δf the wavevector's diagram, shown in figure 1(b), gives us $\eta_0 = \pi\lambda f_0 \Delta f (n_0 v^2)^{-1}$, $\eta_1 \approx -3\eta_0$ and $\eta_2 \approx -7\eta_0$. For this approximation one can restrict oneself by exploiting only the one parameter η_0 for estimating the mismatching effect in the form of the frequency detuning Δf. An illustrative example of numerical simulations related to spatial-frequency distributions for the intensities of all optical components inside a rectangular acoustic pulse in the regime of a four-order light scattering is presented in figure 7 for the case of $q = 4.5$. It is seen that, initially, with $\eta_0 = 0$, well-localized and uniform distributions become broken due to growing the mismatch η_0, i.e. the detuning Δf, or converted into the other multi-wave states of localization.

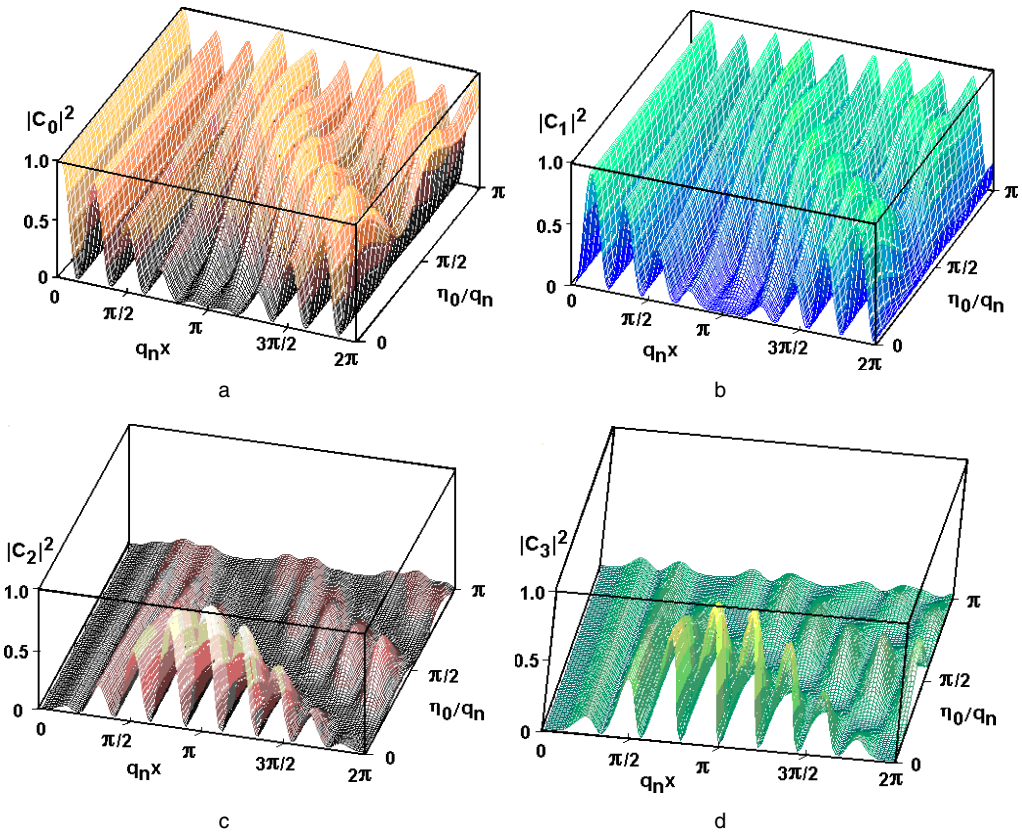

Figure 7. Spatial-frequency distributions for a quartet of optical components in a multi-pulse five-wave weakly coupled state with $q = 4.5$, $I = 1$ and $q_n L \leqslant 2\pi$: an eight-pulse component in the zero order of scattering (a), a nine-pulse component in the first and second orders (b) and (c), an eight-pulse component in the third order (d). The distributions (b), (c) and (d) are completely locked with $\eta_0 = 0$.

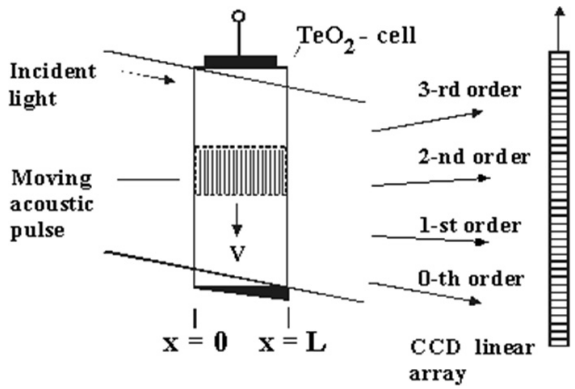

Figure 8. Schematic arrangement of the optical layout for the experimental set-up.

8. Experimental data

A schematic arrangement of the experiment was quite similar to the set-up presented in [1], but in a four-order regime of light scattering, or for the scheme for optical data processing [10]. Our set-up includes a continuous-wave wide aperture laser beam, a non-collinear crystalline cell and the CCD linear array. The corresponding optical layout is shown in figure 8.

The incident light beam was precisely oriented at the Bragg angle θ_0 relative to the acoustic beam to minimize the influence of angular mismatches and thereby to provide just electronic control over measuring contributions of the frequency detuning. Observation of optical components inherent in stationary five-wave weakly coupled acousto-optical states has been carried out with experiments using a cell made of tellurium dioxide crystal oriented along the [001] and [110] axis, respectively, as shown in figure 1(b) ($f_0 = 57.8$ MHz, $v = 0.616$ mm μs^{-1} [5]) on a light wavelength of $\lambda = 0.442$ μm. The Bragg scattering of circularly polarized light, resulting in maximal efficiency of the acousto-optical interaction, was performed without any effect on the acoustic wave that provides the regime of weak coupling. The incident light power from a He–Cd-laser was about 20 mW, while the acoustic beam power was in excess of 4 W. The intensities of the optical components peculiar to five-wave coupled states have been measured as functions of the product $q_n x$ and the frequency detuning Δf on the first interval of localization ($n = 1$). The corresponding digitized oscilloscope traces are presented in figure 8. Because the length of acousto-optical interaction was constant ($L = 1.1$ cm), the power density of the acoustic wave was varied due to varying the applied acoustic power to control the product $q_n x$.

9. Conclusion

Comparing the numerical simulation in figure 7 (where $q = 4.5$) with the oscilloscope traces in figure 9, one

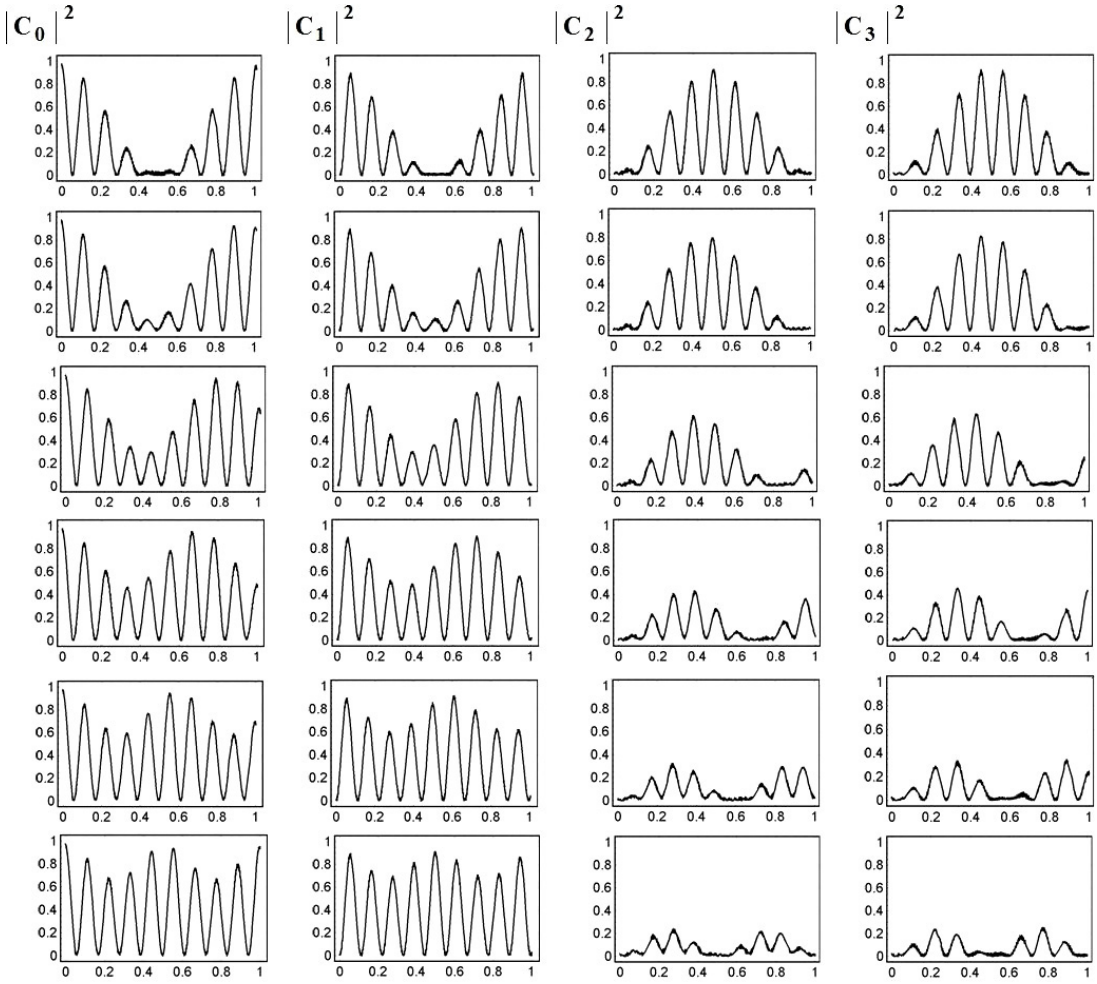

Figure 9. The digitized oscilloscope traces for the intensities $|C_P|^2$ of the optical components in a five-wave coupled state versus the product $q_n x$ at various values of the frequency detuning Δf. The magnitude of Δf is increasing from zero for the upper row through the intermediate values 0.40, 0.75, 1.15 and 1.5 MHz to 2 MHz for the bottom one.

can conclude that the theoretically predicted existence of stationary five-wave weakly coupled acousto-optical states has been experimentally observed at the first interval of localization including $q_n L = 2\pi$. This type of multi-pulse solitary waves has been successfully shaped and identified in a non-collinear acousto-optical cell made of a tellurium dioxide single crystal with the above chosen orientation, which provides very effective light scattering by coherent acoustic waves in the optimized anomalous regime and, together with this, exhibits an appropriate level of light scattering within the normal regime as well. Just the presence of a pair of these regimes simultaneously has led to the results obtained. Moreover, for this purpose it was necessary to estimate critically important contributions from the effect of optical activity in tellurium dioxide. Experimentally observed optical components of five-wave multi-pulse weakly coupled states manifest their stability and tolerance to small frequency detuning. Nevertheless, inserting the growing frequency detuning illustrates the sensitivity of coupled state to mismatches, decreases the efficiency of localization and leads to destroying the localization of the coupled state first of all in the second and third orders of scattering. The last effect takes place because both two- and three-phonon light scattering becomes relatively forbidden well before reaching a sufficiently clearly defined pattern of multi-order scattering processes by itself.

Acknowledgment

This work was financially supported by the CONACyT, Mexico (project no. 61237-F).

References

[1] Shcherbakov A S and Aguirre Lopez A 2003 Shaping the optical components of solitary three-wave weakly coupled states in a two-mode waveguide *Opt. Express* **11** 1643–9 http://www.opticsexpress.org/abstract.cfm?URI=OPEX-11-14-1643

[2] Shcherbakov A S and Aguirre Lopez A 2002 Observation of the optical components inherent in multi-wave non-collinear acousto-optical coupled states *Opt. Express* **10** 1398–403 http://www.opticsexpress.org/abstract.cfm?URI=OPEX-10-24-1398

[3] Korpel A 1997 *Acousto-Optics* (New York: Dekker)

[4] Balakshy V I, Parygin V N and Chirkov L I 1985 *Physical Principles of Acousto-Optics* (Moscow: Radio i Svyaz)
[5] Dmitriev V G, Gurzadyan G G and Nikogosyan D N 1999 *Handbook of Nonlinear Optical Crystals* 3rd edn (Berlin: Springer)
[6] Dixon R W 1967 Acoustic diffraction of light in anisotropic media *IEEE J. Quantum Electron.* **3** 85–93
[7] Wooster W A 1973 *Tensors and Group Theory for the Physical Properties of Crystals* (Oxford: Clarendon)
[8] Voloshinov V and Tchernyatin A 1999 Light diffraction with conservation of optical mode by slow shear wave in paratellurite *Proc. SPIE* **3900** 74–82
[9] Voloshinov V and Tchernyatin A 2000 Bragg isotropic acousto-optic diffraction of light by slow shear acoustic wave in paratellurite *Opt. Spectrosc.* **88** 1000–4
[10] Yu F 2001 *Introduction to Information Optics* (San Diego, CA: Academic)